Compliant Continuum Robots

Subjects: Robotics

Contributor: Shiyao Li

Compliant continuum robots (CCRs) are usually made of elastic materials, including nitinol alloy (NiTi), silicone, rubberand polyamide, etc. They are designed to be slender, i.e., low diameter to length ratio. CCRs have been widely employed in a constraint environment to manipulate tasks, such as minimally invasive cardiac surgery, orthopaedic surgery, endoscopic surgery, bariatric surgeryand the inspection of gas turbine engines, in-situ aero-engine maintenance works.

Keywords: compliant continuum robots ; basic transmission units ; drive systems ; variable stiffness ; sensing

1. Introduction

CCRs have been widely employed in a constraint environment to manipulate tasks, such as minimally invasive cardiac surgery [1], orthopaedic surgery [2][3][4], endoscopic surgery [5], bariatric surgery [6] and the inspection of gas turbine engines [7], in-situ aero-engine maintenance works [8][9][10][11]. Researchers usually classify CCRs in two ways, one is the drive system classification, including tendon-driven robots, cable-driven robots, pneumatic robots, shape-memory-alloy robots. In this paper, we classify the CCRs into two groups, including semi-soft continuum robots and soft continuum robots. sometimes rigid disks or rods are added to increase rigidity [12].

Traditional serial robots consist of rigid links and rigid joints. The comparison between continuum robots and rigid serial robots is shown in **Figure 1**, including the curvature of a robot's shape, size, stiffness and degrees of freedom (DoFs). Semi-soft continuum robots have a minimal scale compared with others; recently a magnetic soft submillimetre scale continuum robot blurs the line between the semi-soft continuum robot and the soft continuum robot, as the magnetic fluid can turn into an elastic solid under a magnetic field [13]. Remaining a high stiffness and a smooth curvature are the aims for designing a continuum robot.

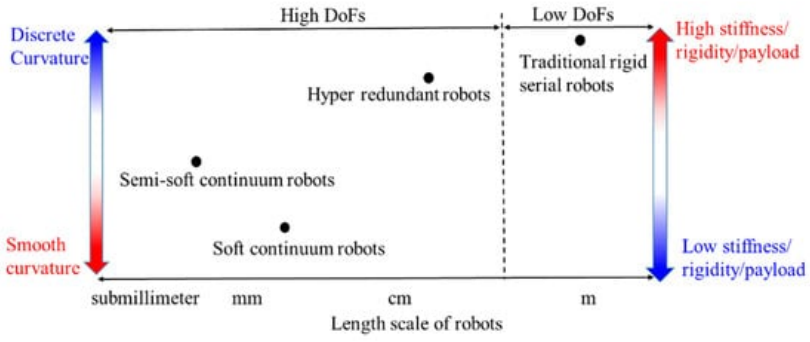

Figure 1. The comparison between CCRs and rigid serial robots.

2. Trends and Classifications of CCRs

The development of CCRs is shown in **Figure 2** from 2000 to 2021. The prototype of CCR was introduced in 2000. It consists of elastic springs, rigid disks and rotational joints, and it is driven by cables [14]. During the following years, there was little research about CCRs from 2002 to 2013, but since 2014, there was a rapid increase in research of CCRs, as shown in **Figure 2**, and the cumulative results can also be seen.

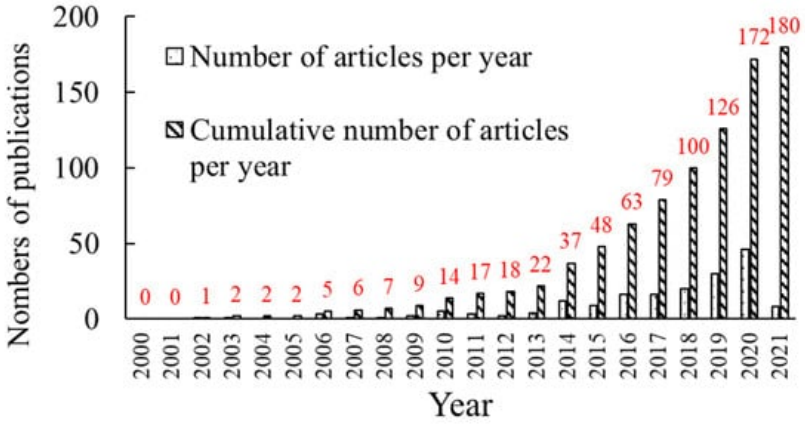

Figure 2. The numbers of publications about CCRs per year.

CCRs are divided into eleven types according to basic transmission units, as shown in **Figure 3**. Soft-tube CCRs belong to soft CCRs, while others belong to semi-soft CCRs. Backbone, soft-tube, concentric-tube and spring CCRs account for a large proportion, followed by compliant-joint, bellow, origami and hybrid CCRs, and the rest of the types are analysed by researchers recently. Their characteristics and problems are summarised in **Table 1**, which are detailed in the following Sections.

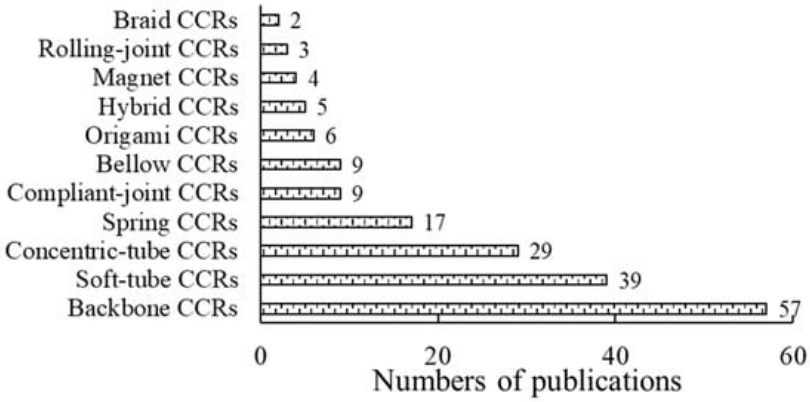

Figure 3. The numbers of publications about different CCRs from the literature review.

Table 1. Descriptions of CCRs.

		Descriptions
Characteristics	basic transmission units	Basic motion units of CCRs.
	drive systems	Actuation force/moment systems, such as the pull-push force, the pneumatic pressure, the hydric pressure and the magnetic force, etc.
	stiffness	Stiffness is the rigidity of a CCR. Including variable stiffness and constant stiffness.
Problems	sensing systems	The accuracy of motions increases with the feedbacks of the sensing systems, including external sensors and intrinsic sensing.
	frictions	Frictions between component units, such as frictions between cable and disk holes.
	buckling	The stiffness suddenly decreases to quasi-zero, when a compressing load acts the CCR.
	singularity	The ill Jacobian matrices between the inputs and outputs.
	twisting	Both torques generated by the CCR weight and the payload influence the tip position.

3. Different Basic Transmission Units and Drive Systems

In this section, the basic transmission units and drive systems are described. The combination of different basic transmission units to form a CCR is called a hybrid CCR, which is also illustrated at the end of this section.

3.1. Basic Transmission Units

3.1.1. Backbone CCRs

The backbone CCRs are shown in **Figure 4**. Most backbones are made of Nickel-Titanium (NiTi) and polypropylene [1]. A centre backbone, secondary backbones (or cables) and several rigid disks are commonly used to form a backbone CCR, shown in **Figure 4**a [15][16][5][17][18][19][20][21][22][23][24][25][26][27][28][29][30][31][32][33]. The central backbone is connected to all the disks. The secondary backbones (or cables) are only connected to the end disk and freely slide in the disk holes for driving the CCR. A backbone CCR also can consist of multi-secondary backbones without a centre backbone, shown in **Figure 4**b [27], which is wearable and used for shoulder recovery. The centre backbone can be an elastic tube [32], an elastic notched tube [34], a half elastic notched tube [35], or an elastic V-shape tube [36][37], shown in **Figure 4**c. The last three tubes can be employed as backbone CCRs without rigid disks.

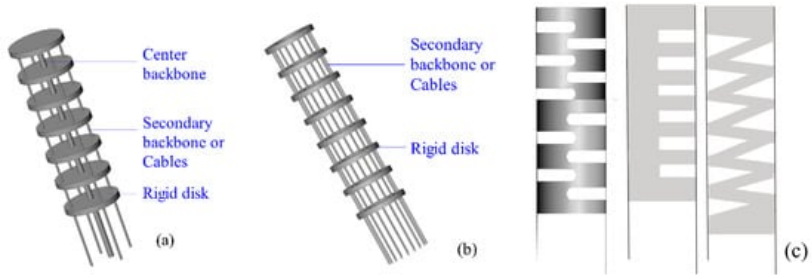

Figure 4. Backbone CCRs: (**a**) A robot with a centre backbone [15][38][39][40], (**b**) a robot without a central backbone [27] and (**c**) notched backbones [37].

The metrics of the backbone are as follows. The distance between two disks can be evenly distributed. The continuous configuration of backbones benefits kinematics modelling. If the backbone has multi-segments, all the endpoints of different segments can be on the same curve, which is easy to correct the curve closing to desired one [19]. The rigidity of the backbone CCR can be adjusted by two methods, including increasing the number of secondary backbones [27] and inserting a rod moving in the centre backbone tube [6][35][41]. The effective bending section of the backbone CCR is controllable by regulating the inserting length of the rod. However, the torsional rigidity of the backbone CCRs is necessary to be enhanced to avoid a low payload and a small stiffness control range [42].

3.1.2. Soft-Tube CCRs

Soft-tube CCRs are the softest type among the CCRs, shown in **Figure 5**. The soft-tube CCR in **Figure 5**a [43][44] has a silicone tube, which is actuated by pneumatic, shape memory alloy and multi-embedded tendons. The soft-tube CCR in **Figure 5**b [45] has a silicone-backbone shape, consisting of a free chamber, six actuation chambers and three driving cables. Its stiffness can be regulated by the pneumatic pressure. The catheter has a sub-millimetre size, shown in **Figure 5**c, and it is usually made of urethane rubber [46] and polymer [47]. The stiffness of the soft-tube CCRs in **Figure 5**a,c is less rigid than that of **Figure 5**b. On the other hand, soft-tube CCRs can be actuated by driving cable, pneumatic champers, shape memory alloy, or electro-polymer. The first two drive systems have higher ratios of power to weight than others. A soft-tube CCR always requires a compliant actuator with a high ratio of power to weight than other CCRs, due to the hyper-redundant DOF [48], so cables and pneumatic champers are commonly used in soft-tube CCR.

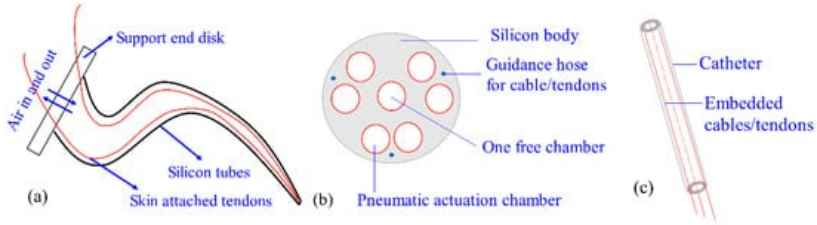

Figure 5. Soft-tube CCRs: (**a**) A silicone-tube CCR [43][44], (**b**) the cross section of another silicone-backbone CCR [45] and (**c**) a catheter CCR [46][47][49][50][51][52].

Soft-tube CCRs have a large elastic deformation and hyper-redundant DoFs. However, their higher compliance reduces the rigidity and positioning accuracy significantly [53]. The lack of rigidity of soft material can result in buckling and strong nonlinearities of the kinematic model. In 2018, Li et al. tried to avoid buckling by optimising controlling models [54]. Soft skin is easy to be torn and punctured, so Wang et al. combined different types of fibres into the silicone to improve their strength and durability [55].

3.1.3. Concentric-Tube CCRs

Concentric tubes are first introduced by Webster et al. [56]. Most tubes are made of superelastic Nitinol, and some of them are made of polyether block amide [57]. They are pre-curved and superelastic, as shown in **Figure 6**. The concentric tubes are inserted inside each other, and they are translated and rotated axially about the concentric axis at the base by tube interactions [58][59]. In this way, the length and curve of the concentric-tube CCR are varied.

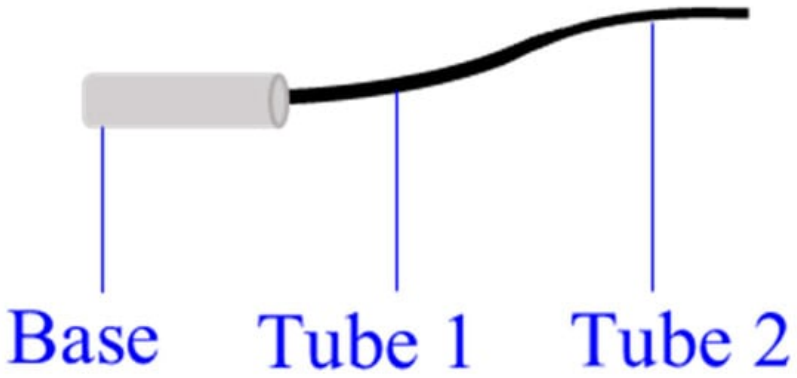

Figure 6. A two-tube concentric-tube CCR [60][61].

The main advantage of concentric-tube CCRs is the sub-millimetre body with enough stiffness, such as a 0.8 mm-diameter tube [62], which leads to a lower infection possibility during the surgery. However, the kinematic analysis is difficult for the special actuation. If the stiffness of these tubes is not comparable, or elastic energy storage occurs in high tube curvatures, the rapid snapping problem may happen [62]. The snaping problem means the CCR snaps quickly from one configuration to another with the energy released suddenly [63]. The concentric-tube CCR should be snap-free to avoid serious harm to patients [64]. In addition, they have limited variations of resultant curvatures as the tubes are pre-curved, so the minimum requirement for the concentric-tube CCRs is to extend into the body smoothly [58][65][66]. The frictions between tubes should not be neglected [64][67][68].

3.1.4. Spring CCRs

Springs can be used in two ways to form a spring CCR, including inner helical springs and outer helical springs, as shown in **Figure 7**. An inner helical spring can be employed as a central backbone [69][70][71][72][73][74][75][76] to evenly distribute disks. An outer spring can be multi-disks to confine cables [77][78][79]. Most spring CCRs are made of steel or NiTi, and they are actuated by cables.

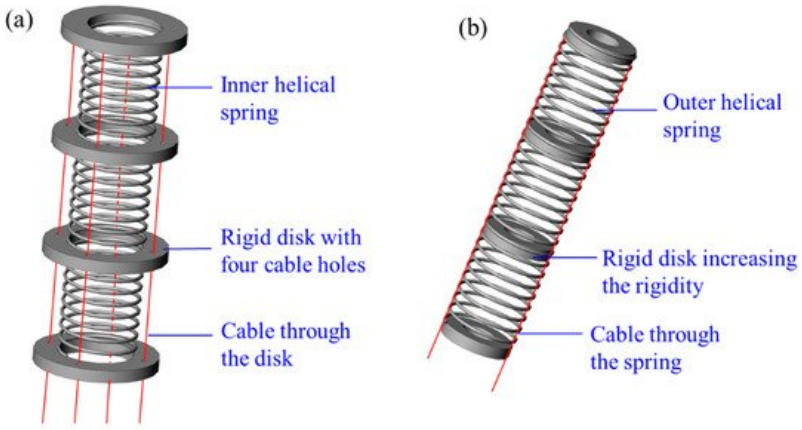

Figure 7. Spring CCRs formed with: (**a**) An inner helical spring [70][80] and (**b**) an outer helical spring [76].

A helical spring has a linear relationship between force and displacement, i.e., an unchanged spring constant, which simplifies the kinematic analysis significantly [70]. The workspace of helical spring CCRs can be expanded by applying a high spring constant. The unwanted extension, uncontrolled compression and singularity can be avoided by applying a low spring constant. The combinations of high and low spring constants can improve torsional rigidity [70]. In addition, spring can also be a buffer to reduce the effects from the environment [11].

3.1.5. Compliant-Joint CCRs

Compliant joints are designed with elastic blades, wire beams, and rigid disks. Blades and wire beams are commonly made of NiTi [12] and polyethylene [81]. Most disks are made of acrylonitrile butadiene styrene (ABS) material for lightweight, and they can constrain cables [82] and increase the rigidity of CCRs [79]. The geometric difference between blade and wire beams is the ratio of width to thickness. The ratio of a blade is larger than 10, and that of a wire beam is equal to 1. **Figure 8** shows the compliant joints, and they can be arranged in series to form a CCR. The compliant-joint CCRs are actuated by cables or backbones, and their curves are varied with the rotations and translations of the elastic blades or wire beams.

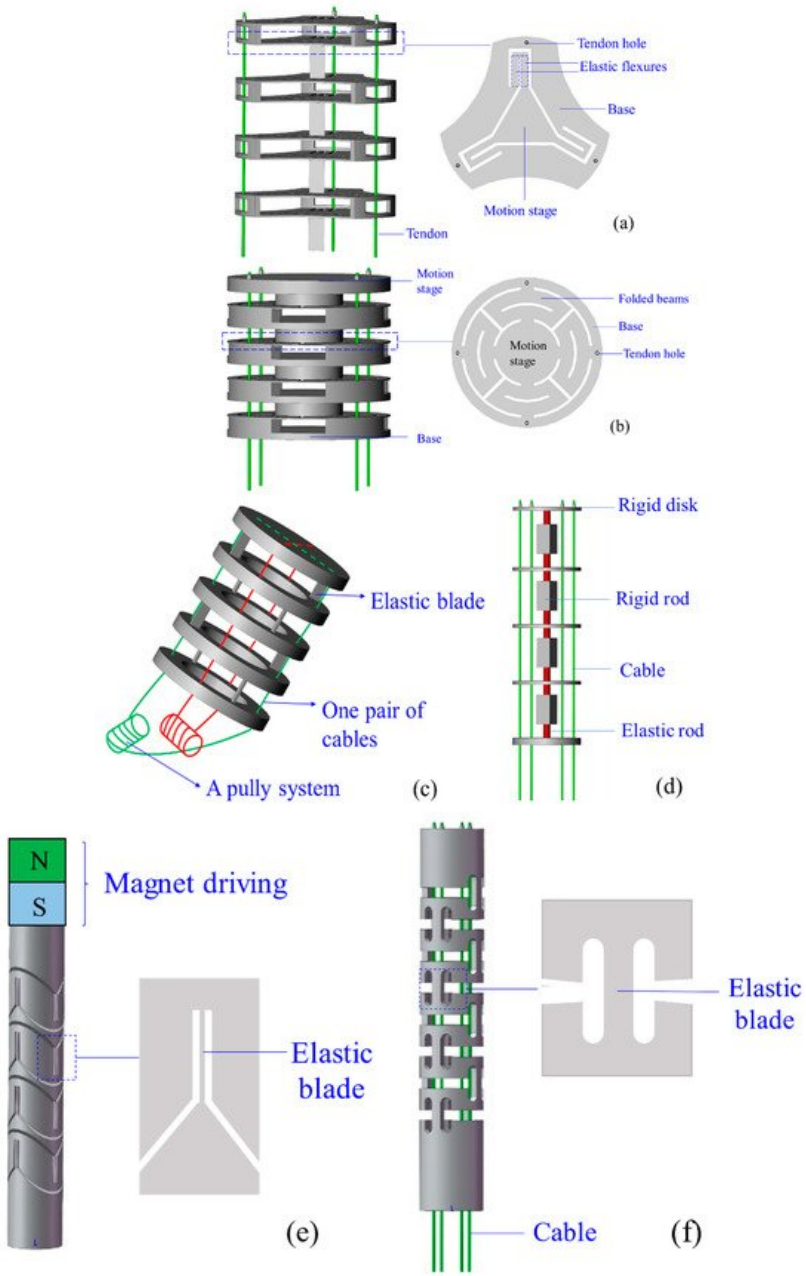

Figure 8. Different compliant joints for the compliant-joint CCRs: (**a**) A planar spring [83], (**b**) a planar spring with minimised parasitic motions [84], (**c**) multi-two-pivots compliant joints [12], (**d**) a compliant joint with two short elastic beams [85], (**e**) multi compliant joints with elastic blades [86] and (**f**) multi compliant joints with round-corner blades [87].

Compared with the rotational symmetric planar spring of Qi et al. [83], shown in **Figure 8**a, the planar spring of Awtar et al. [84] is a mirror-symmetric consisting of eight folded beams, which decreases parasitic motions significantly, shown in **Figure 8**b. Dong et al. presented two types of compliant joint with elastic blades [12] and short beams [85], shown in **Figure 8**c,d, respectively. The compliant-joint CCR formed with the multi-elastic blades can anti twisting compared with the CCR formed with two short beams. Thomas et al. [86] and Zhang et al. [87] designed compliant-joint CCRs with elastic blades, shown in **Figure 8**e,f, respectively.

3.1.6. Bellow CCRs

Figure 9 shows a segment of a bellow CCR. Most bellow CCRs are made of polyamide, and they are actuated by pneumatic or hydraulic pressure with a cables-driven assistant. They can expand or elongate with variable curves as expected by pulling or pushing cables when bellows are filled with air.

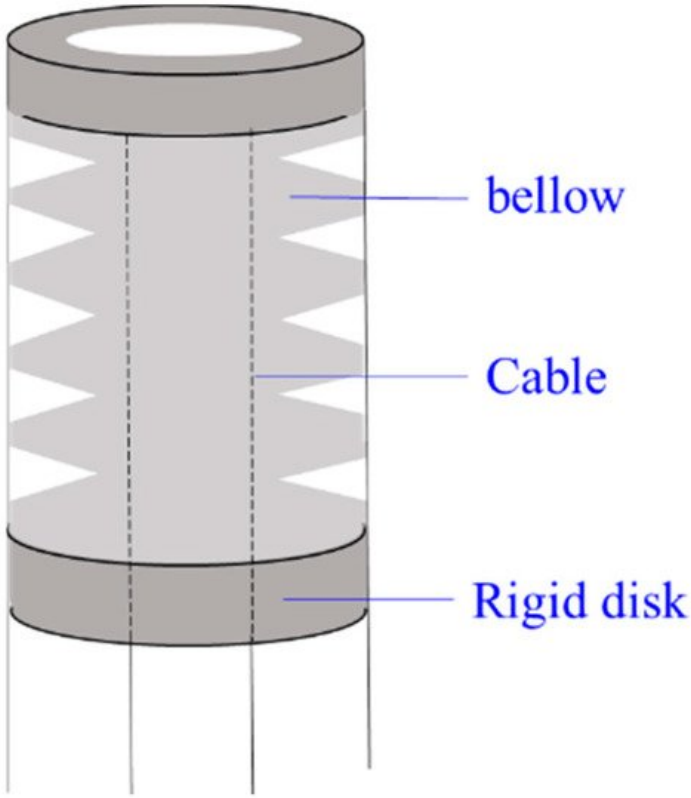

Figure 9. A bellow CCR with cable-driven system [88].

Bellow CCRs are lightweight with a smooth curvature. Another advantage of the bellow is to be employed as an anti-buckling support structure if they are made of NiTi material [31], as NiTi is more rigid than polyamide with enough elasticity. However, bellow CCRs are sometimes unreliable for the non-stationarities during pneumatic or hydraulic actuation [89]. The rigidity of polyamide bellow CCRs is relatively low, so the disks are usually added around the bellow to increase the rigidity [90].

3.1.7. Origami CCRs

Mirror folds, water bomb, folds and reverse folds are basic folds for origami continuum robots. Origami CCRs are made of photopolymer resin or sticky polyamide film [91], which are driven by cables [92][93] as shown in **Figure 10**. Each crease of the origami can be regarded as a 360-degree revolute joint, so Origami CCR has two types of body shapes, including a 2D shape and a 3D shape. They can go through a constrained environment in a smaller 2D shape and morph into a 3D device. If they are applied in minimally invasive surgery, the possibility of infection decreases.

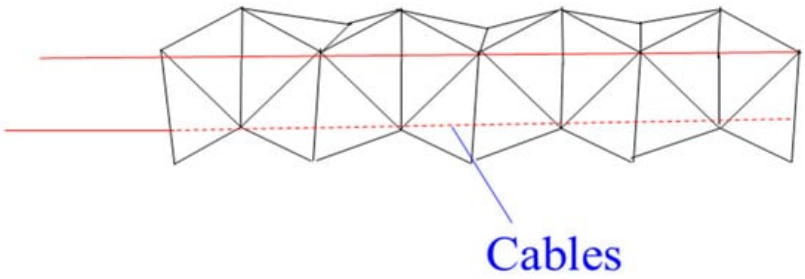

Figure 10. An origami CCR with a cable-driven system [92][93].

3.1.8. Magnet CCRs

Magnetic CCRs are another type of sub-millimetre continuum robots, including permanent-magnet-joint CCRs [94] and magnetic-fluid CCRs [13]. Permanent magnets and magnetic fluids are controlled in the magnet field without any actuation wires. A permanent-magnet-joint CCR is shown in **Figure 11**. The elastic beams are actuated by the interactions of N and S poles. As for magnetic-fluid CCRs, the magnitude of the magnet field affects the viscosity of the magnetic fluid, and the viscosity can be close to the solid viscosity with the increase of the magnitude. Magnet CCRs can also be mounted on medical devices and serving as a guide.

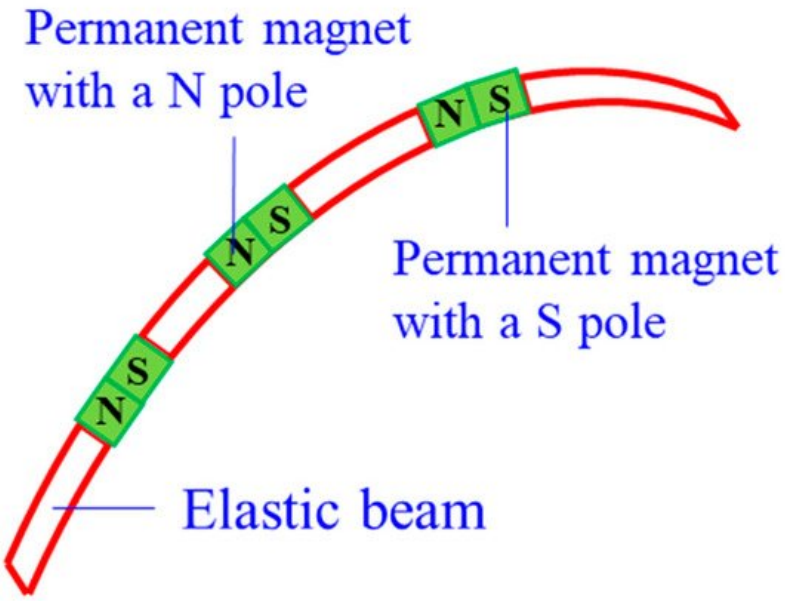

Figure 11. A permanent-magnet CCR [94].

3.1.9. Rolling-Joint CCRs

Rolling-joint CCRs are special for a variable neutral line of the robot, as shown in **Figure 12**. Most rolling joints are made of ABS material to reduce weight. They are actuated by non-circular spur gears [95] as the asymmetric arrangement of rolling joints ($\Delta_x \neq \Delta_y$), and the nonlinear actuating relationship of force and tension is complex to model [96]. Compared with the friction between cables and disk holes, the friction between rolling joints should not be neglected.

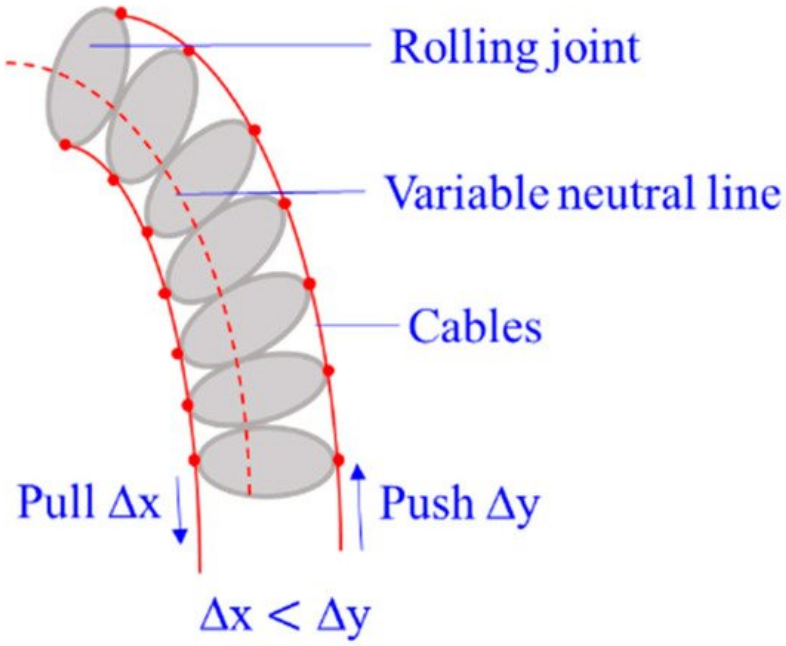

Figure 12. A rolling-joint CCR with a cable-driven system [96].

3.1.10. Braid CCRs

Braid CCRs are inspired by human muscles, which are braided with non-extensible, but flexible fibres in helical arrays. They can extend, contract and bend by actuating embedded radial and longitudinal tendons [97], and they can also be actuated by the pneumatic artificial muscles [98]. They can vary stiffness by antagonistically actuating actuators or increasing the pneumatic pressure. The size of this robot is not miniature, ranging from 10 cm to 27 cm.

3.1.11. Hybrid CCRs

Hybrid CCRs are designed for complementing the shortcomings of a basic unit with the merits of another. **Figure 13** shows the eight types of combinations of the different basic units. Most hybrid CCRs consist of a backbone due to the continuous shape.

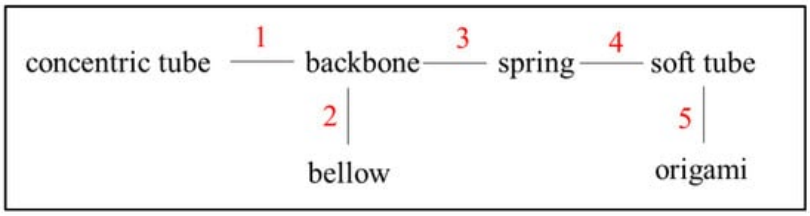

Figure 13. Combinations of different basic transmission units for the hybrid CCRs.

- Backbone-Concentric-Tube CCR

Concentric-tube CCRs can be submillimetre, but they have limited resultant curves and snapping problems. Backbone CCRs are flexible, but the coupling between different segments of a backbone CCR is still a challenge. Wu et al. [99] introduced a backbone-concentric-tube CCRs, whose dexterity is improved and the size is submillimetre. They analysed three combinations of the backbone-concentric-tube robot, as shown in **Figure 14**. The results show that design II can avoid snapping and coupling of different segments compared with others.

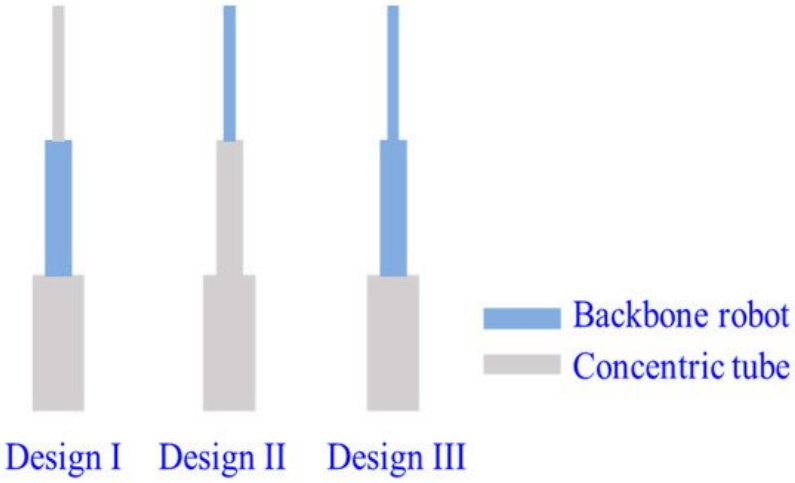

Figure 14. Three designs of the backbone-concentric-tube CCRs [99].

- Backbone-Bellow CCR

The nickel bellow has much higher rigidity than a polyamide bellow. The torsional rigidity of the backbone CCRs is relatively low. Xu et al. introduced a backbone-bellow CCR, whose nickel bellows wrap outside of the backbones [31]. The torsional rigidity of the backbone CCR is enhanced more than four times when a nickel bellow is integrated, and the bending capabilities are not compromised.

- Notched Backbone-Spring CCR

Sharp bending is a challenge for concentric-tube CCRs. To maintain the miniature size and enable sharp bending, Francis et al. [77] introduced a new asymmetric notched backbone-spring CCR, where a helical spring wraps outside of a notched backbone tube, as shown in **Figure 15**. The helical spring is also used to confine the cables.

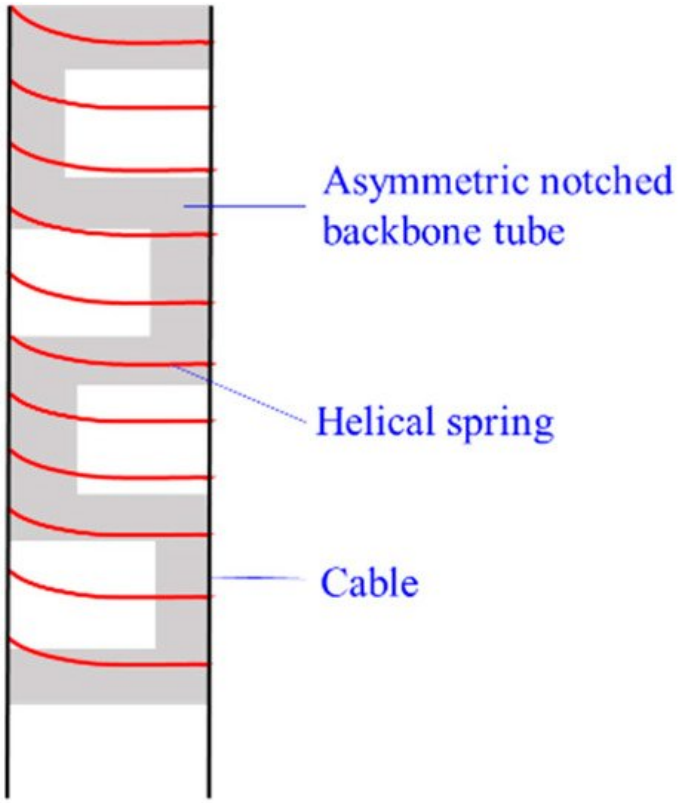

Figure 15. The design of the notched backbone-spring CCRs [77].

- Soft tube-Spring CCR

Xing et al. [100] designed a soft tube-spring CCR, which is super flexible and driven by cables. The spring is employed for confining cables. It is different from the above hybrid CCRs as the spring is in the silicone tube, as shown in **Figure 16**.

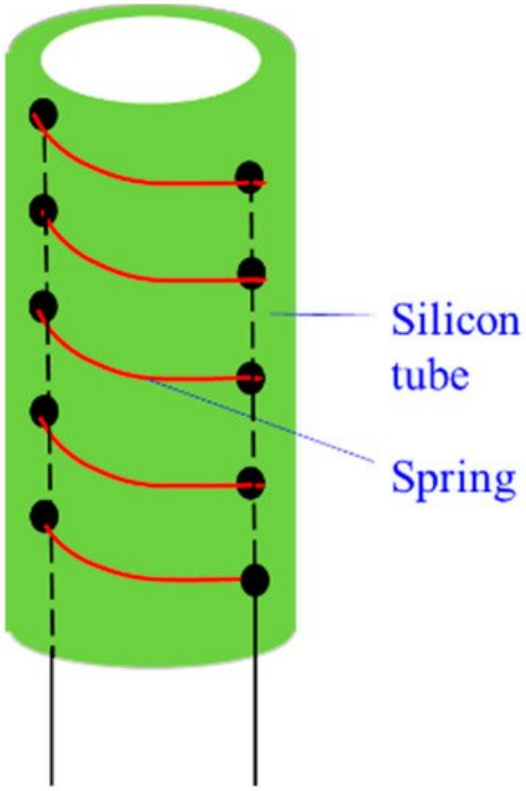

Figure 16. The soft tube-spring CCR [100].

- Soft tube-Origami manipulator

Li et al. presented an origami gripper with soft silicone skin [101]. This gripper is actuated by pneumatic, which can catch different things without shape requirements. This is not a CCR, but it is promising to similarly design a silicone-origami

CCR in the future.

3.2. Drive Systems

Drive systems depend on the basic transmission units of CCRs significantly. Most semi-soft CCRs can be actuated by backbones or cables. The main difference between the backbone-driven and the cable-driven system is as follows. The minimal number of backbones to bend a CCR in any direction is two, but that of cables is three. The reason is a backbone can be compressed and extended, while a cable cannot be compressed. The third actuating backbone or the fourth cable can be employed as the actuation redundancy [102]. A pully system usually actuates one pair of cables, which motivates Dong et al. to present a spooling system (i.e., twin pully systems) to minimise the size of the actuation system significantly [103]. In addition, cable tension is required to be calculated for avoiding cable slack [12], and the backbone-driven system does not have this problem.

Most soft CCRs are actuated by pneumatic and hydraulic pressure, which can modify the length of chambers by varying the air or fluid pressure in the chambers [90]. Cable-driven assistance is usually used for soft CCRs. Shape memory alloy (SMA) and electroactive polymer (EAP) are also used in CCRs. Shape memory alloy can change into a certain shape when the temperature reaches the critical temperature [73][104][105]. Electroactive polymer is a special material that contracts and extends by soft embedded compliant electrodes [106][107]. The advantages and disadvantages of different drive systems are summarised in **Table 2**.

Table 2. Summary of different drive systems.

Drive Systems	Advantages	Disadvantages
Cable/tendon	**Exert large force; easy control; large ratio of power to weight.**	**Cable slack; cable coupling; friction between cables and disks.**
Backbone	**Remote actuation; fewer actuation wires; reduce buckling.**	**Backlash; frictions between actuation lines and conduits; extension and compression of actuating backbones.**
Pneumatic	**Exert large force; variable stiffness by regulating air pressure; large ratio of power to weight.**	**Strong nonlinearities of a kinematic model; not safe enough if the air leak.**
Hydraulic	**Exert large force.**	**The extra weight of fluid; failure of the hydraulic power supply.**
Magnet	**No surface contact; lightweight; Tether-free actuation; sub-millimetre scale.**	**Complex electromagnets control.**
SMA	**Certain shape curvature.**	**Need efficient cooling system; sensitive to environment temperature; slow response speed.**
EPA	**Lightweight; small scale.**	**Low actuation pressure; required high input voltage; limited range motion.**

References

1. Yip, M.C.; Camarillo, D.B. Model-Less Hybrid Position/Force Control: A Minimalist Approach for Continuum Manipulators in Unknown, Constrained Environments. IEEE Robot. Autom. Lett. 2016, 1, 844–851.
2. Alambeigi, F.; Bakhtiarinejad, M.; Sefati, S.; Hegeman, R.; Iordachita, I.; Khanuja, H.; Armand, M. On the Use of a Continuum Manipulator and a Bendable Medical Screw for Minimally Invasive Interventions in Orthopedic Surgery. IEEE Trans. Med. Robot. Bionics 2019, 1, 14–21.
3. Roy, R.; Wang, L.; Simaan, N. Modeling and Estimation of Friction, Extension, and Coupling Effects in Multisegment Continuum Robots. IEEE/ASME Trans. Mechatron. 2016, 22, 909–920.
4. Gao, A.; Murphy, R.J.; Liu, H.; Iordachita, I.I.; Armand, M. Mechanical Model of Dexterous Continuum Manipulators With Compliant Joints and Tendon/External Force Interactions. IEEE/ASME Trans. Mechatron. 2017, 22, 465–475.
5. Kato, T.; Okumura, I.; Song, S.-E.; Golby, A.J.; Hata, N. Tendon-Driven Continuum Robot for Endoscopic Surgery: Preclinical Development and Validation of a Tension Propagation Model. IEEE/ASME Trans. Mechatron. 2015, 20, 2252–2263.

6. Zhang, X.; Li, W.; Chiu, P.W.-Y.; Li, Z. A Novel Flexible Robotic Endoscope With Constrained Tendon-Driven Continuum Mechanism. IEEE Robot. Autom. Lett. 2020, 5, 1366–1372.
7. Dong, X.; Axinte, D.; Palmer, D.; Cobos, S.; Raffles, M.; Rabani, A.; Kell, J. Development of a slender continuum roboti c system for on-wing inspection/repair of gas turbine engines. Robot. Comput. Manuf. 2017, 44, 218–229.
8. Hannan, M.W.; Walker, I.D. Analysis and experiments with an elephant's trunk robot. Adv. Robot. 2001, 15, 847–858.
9. Zheng, T.; Branson, D.T.; Kang, R.; Cianchetti, M.; Guglielmino, E.; Follador, M.; Medrano-Cerda, G.A.; Godage, I.S.; C aldwell, D.G. Dynamic continuum arm model for use with underwater robotic manipulators inspired by octopus vulgaris. In Proceedings of the 2012 IEEE International Conference on Robotics and Automation, Saint Paul, MN, USA, 14–18 May 2012; Institute of Electrical and Electronics Engineers (IEEE): Piscataway, NJ, USA, 2012; pp. 5289–5294.
10. Porter, M.M.; Adriaens, D.; Hatton, R.L.; Meyers, M.A.; McKittrick, J. Why the seahorse tail is square. Science 2015, 34 9.
11. Li, L.; Jin, T.; Tian, Y.; Yang, F.; Xi, F. Design and Analysis of a Square-Shaped Continuum Robot With Better Grasping Ability. IEEE Access 2019, 7, 57151–57162.
12. Dong, X.; Raffles, M.; Cobos-Guzmán, S.; Axinte, D.; Kell, J. A Novel Continuum Robot Using Twin-Pivot Compliant Joi nts: Design, Modeling, and Validation. J. Mech. Robot. 2015, 8, 021010.
13. Kim, Y.; Parada, G.A.; Liu, S.; Zhao, X. Ferromagnetic soft continuum robots. Sci. Robot. 2019, 4, eaax7329.
14. Hannan, M.W.; Walker, I.D. Kinematics and the Implementation of an Elephant's Trunk Manipulator and Other Continuu m Style Robots. J. Robot. Syst. 2003, 20, 45–63.
15. Xu, K.; Simaan, N. An Investigation of the Intrinsic Force Sensing Capabilities of Continuum Robots. IEEE Trans. Robo t. 2008, 24, 576–587.
16. Bajo, A.; Simaan, N. Hybrid motion/force control of multi-backbone continuum robots. Int. J. Robot. Res. 2015, 35, 422 –434.
17. Shen, W.; Yang, G.; Zheng, T.; Wang, Y.; Yang, K.; Fang, Z. An Accuracy Enhancement Method for a Cable-Driven Con tinuum Robot With a Flexible Backbone. IEEE Access 2020, 8, 37474–37481.
18. Langer, M.; Amanov, E.; Burgner-Kahrs, J. Stiffening Sheaths for Continuum Robots. Soft Robot. 2018, 5, 291–303.
19. Ouyang, B.; Liu, Y.; Tam, H.Y.; Sun, N. Design of an Interactive Control System for a Multisection Continuum Robot. IE EE/ASME Trans. Mechatron. 2018, 23, 2379–2389.
20. Case, J.C.; White, E.L.; SunSpiral, V.; Kramer-Bottiglio, R. Reducing Actuator Requirements in Continuum Robots Thro ugh Optimized Cable Routing. Soft Robot. 2018, 5, 109–118.
21. Oliver-Butler, K.; Till, J.; Rucker, C. Continuum Robot Stiffness Under External Loads and Prescribed Tendon Displace ments. IEEE Trans. Robot. 2019, 35, 403–419.
22. Ma, X.; Song, C.; Chiu, W.Y.P.; Li, Z. Autonomous Flexible Endoscope for Minimally Invasive Surgery With Enhanced S afety. IEEE Robot. Autom. Lett. 2019, 4, 2607–2613.
23. Gravagne, I.A.; Rahn, C.D.; Walker, I.D.; Member, S. Large Deflection Dynamics and Control for Planar Continuum Ro bots. IEEE/ASME Trans. Mechatron. 2003, 8, 299–307.
24. Rucker, D.C.; Webster, R.J. Statics and dynamics of continuum robots with general tendon routing and external loadin g. IEEE Trans. Robot. 2011, 27, 1033–1044.
25. Gravagne, I.A.; Walker, I.D. Manipulability, force, and compliance analysis for planar continuum manipulators. IEEE Tra ns. Robot. Autom. 2002, 18, 263–273.
26. Chikhaoui, M.T.; Lilge, S.; Kleinschmidt, S.; Burgner-Kahrs, J. Comparison of Modeling Approaches for a Tendon Actuat ed Continuum Robot With Three Extensible Segments. IEEE Robot. Autom. Lett. 2019, 4, 989–996.
27. Xu, K.; Zhao, J.; Qiu, D.; Wang, Y. A Pilot Study of a Continuum Shoulder Exoskeleton for Anatomy Adaptive Assistanc es. J. Mech. Robot. 2014, 6, 041011.
28. Rone, W.S.; Ben-Tzvi, P. Mechanics Modeling of Multisegment Rod-Driven Continuum Robots. J. Mech. Robot. 2014, 6, 041006.
29. Goldman, R.E.; Bajo, A.; Simaan, N. Compliant Motion Control for Multisegment Continuum Robots With Actuation For ce Sensing. IEEE Trans. Robot. 2014, 30, 890–902.
30. Rone, W.S.; Ben-Tzvi, P. Continuum Robot Dynamics Utilizing the Principle of Virtual Power. IEEE Trans. Robot. 2014, 30, 275–287.

31. Xu, K.; Zhao, J.; Fu, M. Development of the SJTU Unfoldable Robotic System (SURS) for Single Port Laparoscopy. IE EE/ASME Trans. Mechatron. 2014, 20, 2133–2145.

32. Li, Z.; Zin Oo, M.; Nalam, V.; Duc Thang, V.; Ren, H.; Kofidis, T.; Yu, H. Design of a novel flexible endoscope-cardiosco pe. J. Mech. Robot. 2016, 8, 1–9.

33. Yuan, H.; Chiu, P.W.Y.; Li, Z. Shape-Reconstruction-Based Force Sensing Method for Continuum Surgical Robots With Large Deformation. IEEE Robot. Autom. Lett. 2017, 2, 1972–1979.

34. Moses, M.S.; Murphy, R.J.; Kutzer, M.D.M.; Armand, M. Modeling Cable and Guide Channel Interaction in a High-Stren gth Cable-Driven Continuum Manipulator. IEEE/ASME Trans. Mechatron. 2015, 20, 2876–2889.

35. Yoshida, S.; Kanno, T.; Kawashima, K. Surgical Robot With Variable Remote Center of Motion Mechanism Using Flexib le Structure. J. Mech. Robot. 2018, 10, 031011.

36. Du, Z.; Yang, W.; Dong, W. Kinematics Modeling of a Notched Continuum Manipulator. J. Mech. Robot. 2015, 7, 04101 7.

37. Kutzer, M.D.; Segreti, S.M.; Brown, C.Y.; Armand, M.; Taylor, R.H.; Mears, S.C. Design of a new cable-driven manipulat or with a large open lumen: Preliminary applications in the minimally-invasive removal of osteolysis. In Proceedings of t he 2011 IEEE International Conference on Robotics and Automation, Shanghai, China, 9–13 May 2011.

38. He, B.; Wang, Z.; Li, Q.; Xie, H.; Shen, R. An Analytic Method for the Kinematics and Dynamics of a Multiple-Backbone Continuum Robot. Int. J. Adv. Robot. Syst. 2013, 10, 84.

39. Guo, H.; Ju, F.; Cao, Y.; Qi, F.; Bai, D.; Wang, Y.; Chen, B. Continuum robot shape estimation using permanent magnet s and magnetic sensors. Sens. Actuators A Phys. 2019, 285, 519–530.

40. Ouyang, B.; Liu, Y.; Sun, D. Design of a three-segment continuum robot for minimally invasive surgery. Robot. Biomim. 2016, 3, 43.

41. Zhao, B.; Zeng, L.; Wu, Z.; Xu, K. A continuum manipulator for continuously variable stiffness and its stiffness control fo rmulation. Mech. Mach. Theory 2020, 149, 103746.

42. Xu, K.; Fu, M.; Zhao, J. An experimental kinestatic comparison between continuum manipulators with structural variatio ns. In Proceedings of the 2014 IEEE International Conference on Robotics and Automation (ICRA), Hong Kong, China, 31 May–7 June 2014; Institute of Electrical and Electronics Engineers (IEEE): Piscataway, NJ, USA, 2014; pp. 3258–3 264.

43. Zheng, T.; Branson, D.T.; Guglielmino, E.; Kang, R.; Cerda, G.A.M.; Cianchetti, M.; Follador, M.; Godage, I.S.; Caldwell, D.G. Model Validation of an Octopus Inspired Continuum Robotic Arm for Use in Underwater Environments. J. Mech. R obot. 2013, 5, 021004.

44. Renda, F.; Giorelli, M.; Calisti, M.; Cianchetti, M.; Laschi, C. Dynamic Model of a Multibending Soft Robot Arm Driven b y Cables. IEEE Trans. Robot. 2014, 30, 1109–1122.

45. Shiva, A.; Stilli, A.; Noh, Y.; Faragasso, A.; De Falco, I.; Gerboni, G.; Cianchetti, M.; Menciassi, A.; Althoefer, K.; Wurde mann, H.A. Tendon-Based Stiffening for a Pneumatically Actuated Soft Manipulator. IEEE Robot. Autom. Lett. 2016, 1, 632–637.

46. Dalvand, M.M.; Nahavandi, S.; Howe, R.D. An Analytical Loading Model for n-Tendon Continuum Robots. IEEE Trans. Robot. 2018, 34, 1215–1225.

47. Zhang, Z.; Dequidt, J.; Back, J.; Liu, H.; Duriez, C. Motion Control of Cable-Driven Continuum Catheter Robot Through Contacts. IEEE Robot. Autom. Lett. 2019, 4, 1852–1859.

48. Kang, R.; Guglielmino, E.; Zullo, L.; Branson, D.T.; Godage, I.; Caldwell, D.G. Embodiment design of soft continuum ro bots. Adv. Mech. Eng. 2016, 8, 1–13.

49. Camarillo, D.B.; Milne, C.F.; Carlson, C.R.; Zinn, M.R.; Salisbury, J.K. Mechanics Modeling of Tendon-Driven Continuu m Manipulators. IEEE Trans. Robot. 2008, 24, 1262–1273.

50. Hasanzadeh, S.; Janabi-Sharifi, F. An Efficient Static Analysis of Continuum Robots. J. Mech. Robot. 2014, 6, 031011.

51. Lotfavar, A.; Hasanzadeh, S.; Janabi-Sharifi, F. Cooperative Continuum Robots: Concept, Modeling, and Workspace An alysis. IEEE Robot. Autom. Lett. 2017, 3, 426–433.

52. Yu, B.; Fernández, J.D.G.; Tan, T. Probabilistic Kinematic Model of a Robotic Catheter for 3D Position Control. Soft Rob ot. 2019, 6, 184–194.

53. Kang, R.; Guo, Y.; Chen, L.; Branson, D.T.; Dai, J.S. Design of a Pneumatic Muscle Based Continuum Robot With Emb edded Tendons. IEEE/ASME Trans. Mech. 2016, 22, 751–761.

54. Li, M.; Kang, R.; Branson, D.T.; Dai, J.S. Model-Free Control for Continuum Robots Based on an Adaptive Kalman Filte r. IEEE/ASME Trans. Mechatron. 2017, 23, 286–297.

55. Wang, Y.; Gregory, C.; Minor, M.A. Improving Mechanical Properties of Molded Silicone Rubber for Soft Robotics Throu gh Fabric Compositing. Soft Robot. 2018, 5, 272–290.

56. Webster, R.J.; Okamura, A.M.; Cowan, N.J. Toward Active Cannulas: Miniature Snake-Like Surgical Robots. In Procee dings of the 2006 IEEE/RSJ International Conference on Intelligent Robots and Systems, Beijing, China, 9–15 October 2006; pp. 2857–2863.

57. Morimoto, T.K.; Okamura, A.M. Design of 3-D Printed Concentric Tube Robots. IEEE Trans. Robot. 2016, 32, 1419–14 30.

58. Bergeles, C.; Gosline, A.H.; Vasilyev, N.V.; Codd, P.J.; Del Nido, P.J.; Dupont, P.E. Concentric Tube Robot Design and Optimization Based on Task and Anatomical Constraints. IEEE Trans. Robot. 2015, 31, 67–84.

59. Dupont, P.E.; Lock, J.; Itkowitz, B.; Butler, E.J. Design and Control of Concentric-Tube Robots. IEEE Trans. Robot. 201 0, 26, 209–225.

60. Iyengar, K.; Dwyer, G.; Stoyanov, D. Investigating exploration for deep reinforcement learning of concentric tube robot c ontrol. Int. J. Comput. Assist. Radiol. Surg. 2020, 15, 1157–1165.

61. Su, H.; Li, G.; Rucker, D.C.; Iii, R.J.W.; Fischer, G.S. A Concentric Tube Continuum Robot with Piezoelectric Actuation f or MRI-Guided Closed-Loop Targeting. Ann. Biomed. Eng. 2016, 44, 2863–2873.

62. Webster, I.R.J.; Romano, J.M.; Cowan, N.J. Mechanics of Precurved-Tube Continuum Robots. IEEE Trans. Robot. 200 9, 25, 67–78.

63. Hendrick, R.J.; Gilbert, H.B.; Webster, R.J. Designing snap-free concentric tube robots: A local bifurcation approach. In Proceedings of the 2015 IEEE International Conference on Robotics and Automation (ICRA), Seattle, WA, USA, 25–30 May 2015; pp. 2256–2263.

64. Gilbert, H.B.; Hendrick, R.J.; Iii, R.J.W. Elastic Stability of Concentric Tube Robots: A Stability Measure and Design Tes t. IEEE Trans. Robot. 2016, 32, 20–35.

65. Rucker, D.C.; Webster, I.R.J.; Chirikjian, G.S.; Cowan, N.J. Equilibrium Conformations of Concentric-tube Continuum R obots. Int. J. Robot. Res. 2010, 29, 1263–1280.

66. Kudryavtsev, A.V.; Chikhaoui, M.T.; Liadov, A.; Rougeot, P.; Spindler, F.; Rabenorosoa, K.; Burgner-Kahrs, J.; Tamadazt e, B.; Andreff, N. Eye-in-Hand Visual Servoing of Concentric Tube Robots. IEEE Robot. Autom. Lett. 2018, 3, 2315–23 21.

67. Vandini, A.; Bergeles, C.; Glocker, B.; Giataganas, P.; Yang, G.-Z. Unified Tracking and Shape Estimation for Concentri c Tube Robots. IEEE Trans. Robot. 2017, 33, 901–915.

68. Xu, R.; Yurkewich, A.; Patel, R.V. Curvature, Torsion, and Force Sensing in Continuum Robots Using Helically Wrapped FBG Sensors. IEEE Robot. Autom. Lett. 2016, 1, 1052–1059.

69. Haraguchi, D.; Kanno, T.; Tadano, K.; Kawashima, K. A Pneumatically Driven Surgical Manipulator With a Flexible Dista l Joint Capable of Force Sensing. IEEE/ASME Trans. Mechatron. 2015, 20, 2950–2961.

70. Li, M.; Kang, R.; Geng, S.; Guglielmino, E. Design and control of a tendon-driven continuum robot. Trans. Inst. Meas. C ontrol. 2018, 40, 3263–3272.

71. Yoon, H.-S.; Jeong, J.H.; Yi, B.-J. Image-Guided Dual Master–Slave Robotic System for Maxillary Sinus Surgery. IEEE Trans. Robot. 2018, 34, 1098–1111.

72. Santiago, J.L.C.; Godage, I.S.; Gonthina, P.; Walker, I.D. Soft Robots and Kangaroo Tails: Modulating Compliance in C ontinuum Structures Through Mechanical Layer Jamming. Soft Robot. 2016, 3, 54–63.

73. Kim, Y.; Cheng, S.S.; Diakite, M.; Gullapalli, R.P.; Simard, J.M.; Desai, J.P. Toward the Development of a Flexible Meso scale MRI-Compatible Neurosurgical Continuum Robot. IEEE Trans. Robot. 2017, 33, 1386–1397.

74. Gao, A.; Zou, Y.; Wang, Z.; Liu, H. A General Friction Model of Discrete Interactions for Tendon Actuated Dexterous Ma nipulators. J. Mech. Robot. 2017, 9, 041019.

75. Frazelle, C.G.; Kapadia, A.D.; Walker, I.D. A Haptic Continuum Interface for the Teleoperation of Extensible Continuum Manipulators. IEEE Robot. Autom. Lett. 2020, 5, 1875–1882.

76. Feng, F.; Hong, W.; Xie, L. Design of 3D-Printed Flexible Joints With Presettable Stiffness for Surgical Robots. IEEE Ac cess 2020, 8, 79573–79585.

77. Francis, P.; Eastwood, K.W.; Bodani, V.; Price, K.; Upadhyaya, K.; Podolsky, D.; Azimian, H.; Looi, T.; Drake, J. Miniatur ized Instruments for the da Vinci Research Kit: Design and Implementation of Custom Continuum Tools. IEEE Robot. A

utom. Mag. 2017, 24, 24–33.

78. Thuruthel, T.G.; Falotico, E.; Manti, M.; Pratesi, A.; Cianchetti, M.; Laschi, C. Learning Closed Loop Kinematic Controlle rs for Continuum Manipulators in Unstructured Environments. Soft Robot. 2017, 4, 285–296.
79. Frazelle, C.G.; Kapadia, A.; Walker, I. Developing a Kinematically Similar Master Device for Extensible Continuum Rob ot Manipulators. ASME J. Mech. Robot. 2018, 10, 025005.
80. Yeshmukhametov, A.; Buribayev, Z.; Amirgaliyev, Y.; Ramakrishnan, R.R. Modeling and Validation of New Continuum R obot Backbone Design With Variable Stiffness Inspired from Elephant Trunk. IOP Conf. Series Mater. Sci. Eng. 2018, 4 17, 012010.
81. Hao, G.; Dai, F.; He, X.; Liu, Y. Design and analytical analysis of a large-range tri-symmetrical 2R1T compliant mechani sm. Microsyst. Technol. 2017, 23, 4359–4366.
82. Simaan, N.; Taylor, R.; Flint, P. A dexterous system for laryngeal surgery. In Proceedings of the IEEE International Conf erence on Robotics and Automation, 2004. ICRA '04. 2004, New Orleans, LA, USA, 26 April–1 May 2004.
83. Qi, P.; Qiu, C.; Liu, H.; Dai, J.S.; Seneviratne, L.; Althoefer, K.A. A Novel Continuum Manipulator Design Using Serially Connected Double-Layer Planar Springs. IEEE/ASME Trans. Mechatron. 2015, 21, 1281–1292.
84. Awtar, S.; Slocum, A.H. Flexure systems based on a symmetric diaphragm flexure. In Proceedings of the ASPE 2005 A nnual Meeting, Chicago, IL, USA, 10–14 September 2005.
85. Dong, X.; Raffles, M.; Guzman, S.C.; Axinte, D.; Kell, J. Design and analysis of a family of snake arm robots connected by compliant joints. Mech. Mach. Theory 2014, 77, 73–91.
86. Thomas, T.L.; Venkiteswaran, V.K.; Ananthasuresh, G.K.; Misra, S. A Monolithic Compliant Continuum Manipulator: A P roof-of-Concept Study. J. Mech. Robot. 2020, 12, 1–11.
87. Zhang, T.; Ping, Z.; Zuo, S. Miniature Continuum Manipulator with 3-DOF Force Sensing for Retinal Microsurgery. J. M ech. Robot. 2021, 1–34.
88. Walker, I.D. Continuous Backbone 'Continuum' Robot Manipulators. ISRN Robot. 2013, 2013, 1–19.
89. Rolf, M.; Steil, J.J. Efficient Exploratory Learning of Inverse Kinematics on a Bionic Elephant Trunk. IEEE Trans. Neural Netw. Learn. Syst. 2014, 25, 1147–1160.
90. Bailly, Y.; Amirat, Y.; Fried, G. Modeling and Control of a Continuum Style Microrobot for Endovascular Surgery. IEEE Tr ans. Robot. 2011, 27, 1024–1030.
91. Kim, S.-J.; Lee, D.-Y.; Jung, G.-P.; Cho, K.-J. An origami-inspired, self-locking robotic arm that can be folded flat. Sci. R obot. 2018, 3, eaar2915.
92. Edmondson, B.J.; Bowen, L.A.; Grames, C.L.; Magleby, S.P.; Howell, L.L.; Bateman, T.C. Oriceps: Origami-Inspired For ceps. In Proceedings of the ASME 2013 Conference on Smart Materials, Adaptive Structures and Intelligent Systems. Volume 1: Development and Characterization of Multifunctional Materials; Modeling, Simulation and Control of Adaptive Systems; Integrated System Design and Implementation, Snowbird, UT, USA, 16–18 September 2013.
93. Zhang, K.; Qiu, C.; Dai, J.S. An Extensible Continuum Robot With Integrated Origami Parallel Modules. J. Mech. Robo t. 2016, 8, 031010.
94. Edelmann, J.; Petruska, A.J.; Nelson, B.J. Magnetic control of continuum devices. Int. J. Robot. Res. 2017, 36, 68–85.
95. Suh, J.-W.; Kim, K.-Y.; Jeong, J.-W.; Lee, J.-J. Design Considerations for a Hyper-Redundant Pulleyless Rolling Joint With Elastic Fixtures. IEEE/ASME Trans. Mechatron. 2015, 20, 2841–2852.
96. Kim, Y.-J.; Cheng, S.; Kim, S.; Iagnemma, K. A Stiffness-Adjustable Hyperredundant Manipulator Using a Variable Neut ral-Line Mechanism for Minimally Invasive Surgery. IEEE Trans. Robot. 2014, 30, 382–395.
97. Hassan, T.; Cianchetti, M.; Mazzolai, B.; Laschi, C.; Dario, P. Active-Braid, a Bioinspired Continuum Manipulator. IEEE Robot. Autom. Lett. 2017, 2, 2104–2110.
98. Felt, W.; Chin, K.Y.; Remy, C.D. Contraction Sensing With Smart Braid McKibben Muscles. IEEE/ASME Trans. Mechatr on. 2016, 21, 1201–1209.
99. Wu, L.; Crawford, R.; Roberts, J. Dexterity Analysis of Three 6-DOF Continuum Robots Combining Concentric Tube Me chanisms and Cable-Driven Mechanisms. IEEE Robot. Autom. Lett. 2016, 2, 514–521.
100. Xing, Z.; Wang, F.; Ji, Y.; McCoul, D.; Wang, X.; Zhao, J. A Structure for Fast Stiffness-Variation and Omnidirectional-St eering Continuum Manipulator. IEEE Robot. Autom. Lett. 2021, 6, 755–762.
101. Li, S.; Stampfli, J.J.; Xu, H.J.; Malkin, E.; Diaz, E.V.; Rus, D.; Wood, R.J. A vacuum-driven origami 'magic-ball' soft grip per. In Proceedings of the 2019 International Conference on Robotics and Automation (ICRA), Montreal, QC, Canada, 20–24 May 2019; pp. 7401–7408.

102. Simaan, N. Snake-Like Units Using Flexible Backbones and Actuation Redundancy for Enhanced Miniaturization. In Proceedings of the 2005 IEEE International Conference on Robotics and Automation, Barcelona, Spain, 18–22 April 2005; pp. 3012–3017.
103. Dong, X.; Palmer, D.; Axinte, D.; Kell, J. In-situ repair/maintenance with a continuum robotic machine tool in confined space. J. Manuf. Process. 2019, 38, 313–318.
104. Kim, Y.; Cheng, S.S.; Desai, J.P. Active Stiffness Tuning of a Spring-Based Continuum Robot for MRI-Guided Neurosurgery. IEEE Trans. Robot. 2017, 34, 18–28.
105. Yang, C.; Geng, S.; Walker, I.; Branson, D.T.; Liu, J.; Dai, J.S.; Kang, R. Geometric constraint-based modeling and analysis of a novel continuum robot with Shape Memory Alloy initiated variable stiffness. Int. J. Robot. Res. 2020, 39, 1620–1634.
106. Pelrine, R.E.; Kornbluh, R.D.; Joseph, J.P.; International, S.R.I.; Ave, R.; Park, M. Electrostriction of polymer dielectrics with compliant electrodes as a means of actuation. Sens. Actuators A Phys. 1998, 4247, 77–85.
107. Moghadam, A.A.A.; Torabi, K.; Kaynak, A.; Alam, M.N.H.Z.; Kouzani, A.; Mosadegh, B. Control-Oriented Modeling of a Polymeric Soft Robot. Soft Robot. 2016, 3, 82–97.
